

Effective polysulfides trapping polar interlayer for high rate Li-S batteries

Saravanan Karuppiah,^{a,b} Balakumar Kalimuthu,^{a,b} Mohammed Azeezulla Nazrulla,^{a,b} Sailaja Krishnamurthy,^{b,c} and Kalaiselvi Nallathamby*^{a,b}

^aCSIR-Central Electrochemical Research Institute, Karaikudi-630 003, Tamilnadu, India.

^bAcSIR – Academy of Scientific & Innovative Research.

^cCSIR-National Chemical Laboratory, Pune-411008, India.

Experimental

Materials

All the chemicals were obtained from Sigma-Aldrich/Alfa Aesar. Deionized water with a conductivity of 0.055 $\mu\text{S cm}^{-1}$ was used. All the chemicals were used without any further purification.

Synthesis of CNF

CNF has been synthesized by chemical blown method [using hexamethylenetetramine (HMT) as C and N precursor and ammonium chloride (NH_4Cl) as blowing agent] and subsequently activated with potassium hydroxide (KOH). In a typical synthesis, 1:1 wt% of HMT and NH_4Cl were mixed together, transferred to an alumina boat and annealed in a tubular furnace at 700 °C with a heating rate of 2° C per minute for 6 h under N_2 atmosphere.²⁷ Subsequently, the obtained black foamy mass of chemically blown carbon nitride after cooling to room temperature was ground well and mixed with KOH (1:1 wt.%) in EtOH medium. Further, the mixture was stirred for 16 h at room temperature and the excess EtOH was dried at 70 °C for 5 h. The resultant product was transferred to an alumina boat and activated further at 700 °C for 6 h with a heating rate of 2 °C per minute in a tubular furnace under N_2 atmosphere. The material thus obtained was added

with 1 N HCl and stirred for about 12 h to remove the impurities and the residual potassium. Finally, the obtained powder was washed several times with water and dried at 120 °C to obtain microporous CNF as the final product.²⁷

Synthesis of CNF-X composites

Series of CNF-sulfur composites (designated as CNF-X where X = 40, 50, 60 and 70 wt.% of sulfur) were obtained by melt diffusion strategy. The required amount of sulfur was mixed with CNF and kept at 280 °C for 12 h to obtain melt diffused CNF-X composites. Subsequently, the product was cooled down to room temperature at a cooling rate of 2 °C min⁻¹.

Electrode fabrication and coin cell assembly

To prepare the electrode, the CNF-sulfur composite (CNF-X) was mixed with super-P carbon black and polyvinylidene fluoride binder in the weight ratio of 80:10:10 and N-methyl-2-pyrrolidone was used to obtain a slurry. This slurry was coated over an aluminium foil current collector and dried at 60 °C for 12 h. The mass loading of the coated electrode is calculated to be around 1.5-2 mg (with respect to sulfur) per 1.87 cm². For interlayer studies, the slurry (made out of 80 wt.% CNF, 10 wt.% super-P carbon and 10 wt.% PVdF using NMP as solvent) was coated over the celgard separator (MTI, Corporation), which was dried at 60 °C, prior to its deployment as interlayer. The electrochemical performance of CNF-X was studied using 2032 coin cells (M/s. Hohsen Corporation) by deploying the electrode punched out from the coated foil with a diameter of 14.45 mm as the working electrode. Lithium metal was used as the counter and reference electrode and Celgard-2400 (Monolayer Polypropylene) was used as the separator. Physical parameters of Celgard-2400: Thickness: 25 µm; JIS Gurley: 620 seconds; Porosity: 41%; PP Pore Size: 0.043 µm; TD Shrinkage @ 90° C/1 hour: 0%; MD Shrinkage @ 90° C/1 hour: ≤ 5%; Puncture Strength: ≥ 450 grams; TD Tensile Strength: 140 kgf/cm² and MD Tensile Strength: 1420

kgf/cm². The electrolyte used was 1 M lithium bis(trifluoromethanesulfonyl)imide and 0.1 M lithium nitrate, dissolved in a co-solvent of 1,3-dioxolane and 1,2-dimethoxyethane (1:1 v/v ratio). The cells were assembled in an Argon-filled glove box, crimp sealed and kept for ageing (24h), prior to electrochemical characterization.

Characterization

The prepared CNF and CNFS composites (CNF-X) were investigated using the following characterization studies. XRD was recorded with a Bruker D8 Advance X-ray diffractometer (XRD) using Ni-filtered Cu K_α radiation. TGA and Raman spectral studies of CNF-X were performed using TA Instruments SDT Q600 thermogravimetric analyser and a Renishawin Raman Microscope using He–Ne LASER at an exciting wavelength of 633 nm respectively. N₂ adsorption/desorption isotherm was obtained from Quantachrome Instruments version 11.02 and XPS results are obtained from a MULTILAB 2000 Base system. Morphology changes after sulfur loading and elemental mapping were studied using Gemini Field Emission Scanning Electron Microscopy (FESEM), Tecnai 20 G2 (FEI make) High Resolution Transmission Electron Microscopy (HRTEM) and STEM JEOL, JEM 2100 respectively. Cyclic Voltammetry (CV) and impedance measurements were carried out using a VMP3 multichannel potentiostat–galvanostat system (Biologic Science Instrument). CV of CNFS composites recorded at a scan rate of 0.1 mV s⁻¹ in the potential region of 1.5–3.0 vs. Li⁺/Li. The Nyquist plots were recorded potentiostatically by applying an AC voltage of 10 mV amplitude in the 100 kHz to 10 mHz frequency range. Charge–discharge studies were carried out using Arbin charge–discharge cyler. The fitted equivalent circuit contains various circuit elements such as R₁, Q₁//R₂, Q₂//R₃ and W. Here, R₁ is the electrolyte resistance, R₃ is the surface resistance of lithium and CNFS composite cathodes, R₂

is the charge transfer resistance, Q_1 and Q_2 are the constant phase elements, and W is the Warburg impedance.

Theoretical Methodology

All the Density functional theory (DFT) calculations were performed using plane-wave (PW) basis set and projector augmented wave method (PAW) as implemented in Vienna *ab-initio* simulation package (VASP).^{51,52} Exchange and correlation terms were treated with Perdew–Burke–Ernzerhof (PBE) functional within the Generalized gradient approximation (GGA).⁵³ In order to account for the long-range Van der Waals dispersion forces, Grimme’s DFT-D2 approach has been deployed along with PBE. A 3x3 supercell of CNF with 63 atoms (Lattice parameters: $a=b=14.346 \text{ \AA}$, and $c=20 \text{ \AA}$, $\alpha=\beta=90^\circ$, and $\gamma=120^\circ$) was constructed from the optimized unit cell of CNF.⁵⁴ To avoid the interaction between periodic images related to the calculations of CNF and CNF-Li₂S₆ composite, a vacuum thickness of 20 \AA was introduced perpendicular to the basal plane of CNF. A PW cut-off of 520 eV was used for all the calculations to ensure complete convergence. Brillouin zone sampling was carried out with 2x2x1 Monkhorst-Pack grid for the optimizations of CNF and CNF-Li₂S₆ composite and for Density of states (DOS), 8x8x1 Monkhorst-Pack grid was used. All the geometries were relaxed until the total energy was converged to 10^{-6} eV per atom and the maximum force to lower than 0.001 eV/ \AA . For the calculations of Li₂S₆ cluster, a large cubical box of size 15 \AA x 15 \AA x 15 \AA with gamma point to sample the Brillouin zone with 1x1x1 k-point sampling was deployed. Bader charge population scheme was utilized for the calculations of charges and charge-transfer analysis.^{55,56}

The binding energy of Li₂S₆ ($E_{B,E}$) with CNF was calculated using the following equation;

$$E_{B,E} = E_{g - CNF + Li_2S_6} - (E_{g - CNF} + E_{Li_2S_6}) \quad \text{eq. 1}$$

Where, $E_{g-CNF+Li_2S_6}$ is the total energy of the composite, E_{g-CNF} is the total energy of the g-CNF, and $E_{Li_2S_6}$ is the total energy of the cluster. The negative value of $E_{B.E}$ indicates the feasibility of chemisorption.

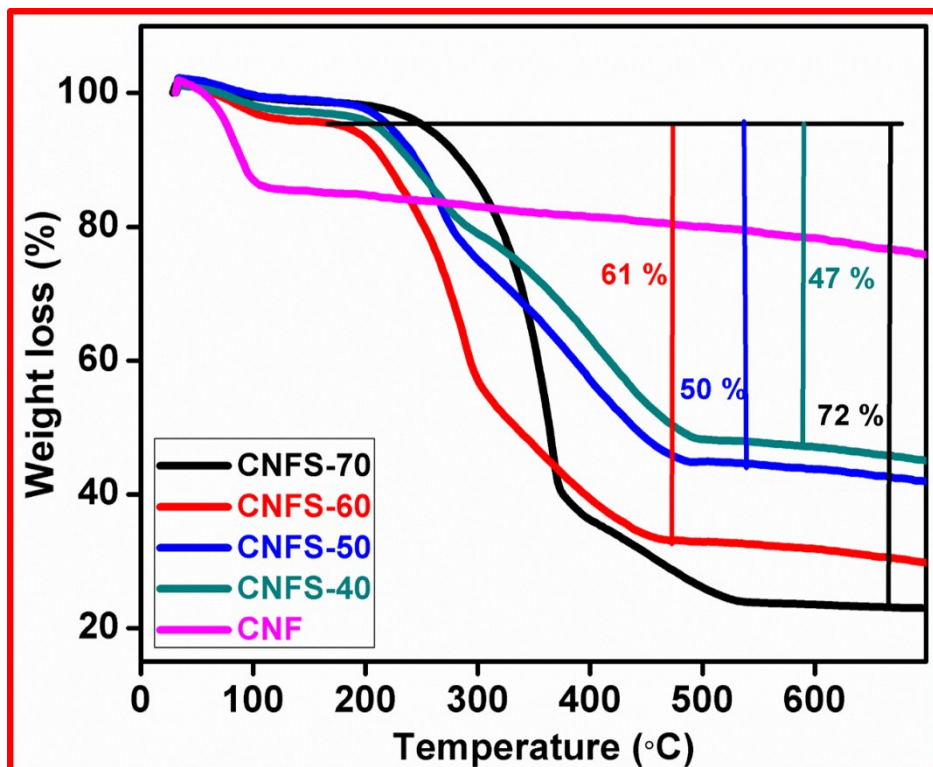


Figure S1. Thermogravimetric analysis of CNF and CNFS-X (X = 40, 50, 60 and 70) composites.

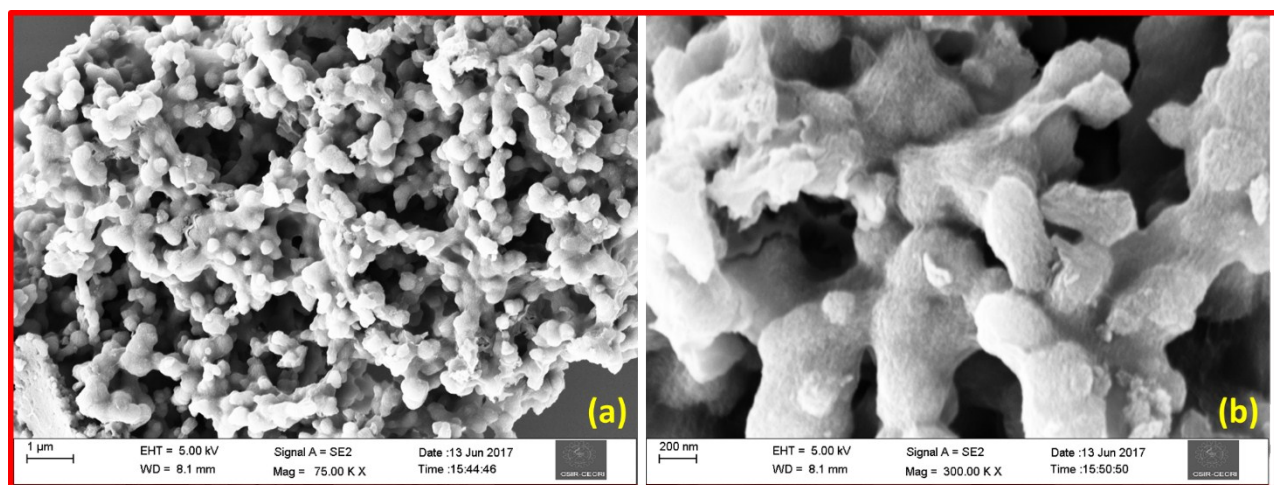


Figure S2. Low (a) and high magnification (b) FESEM images of CNF.

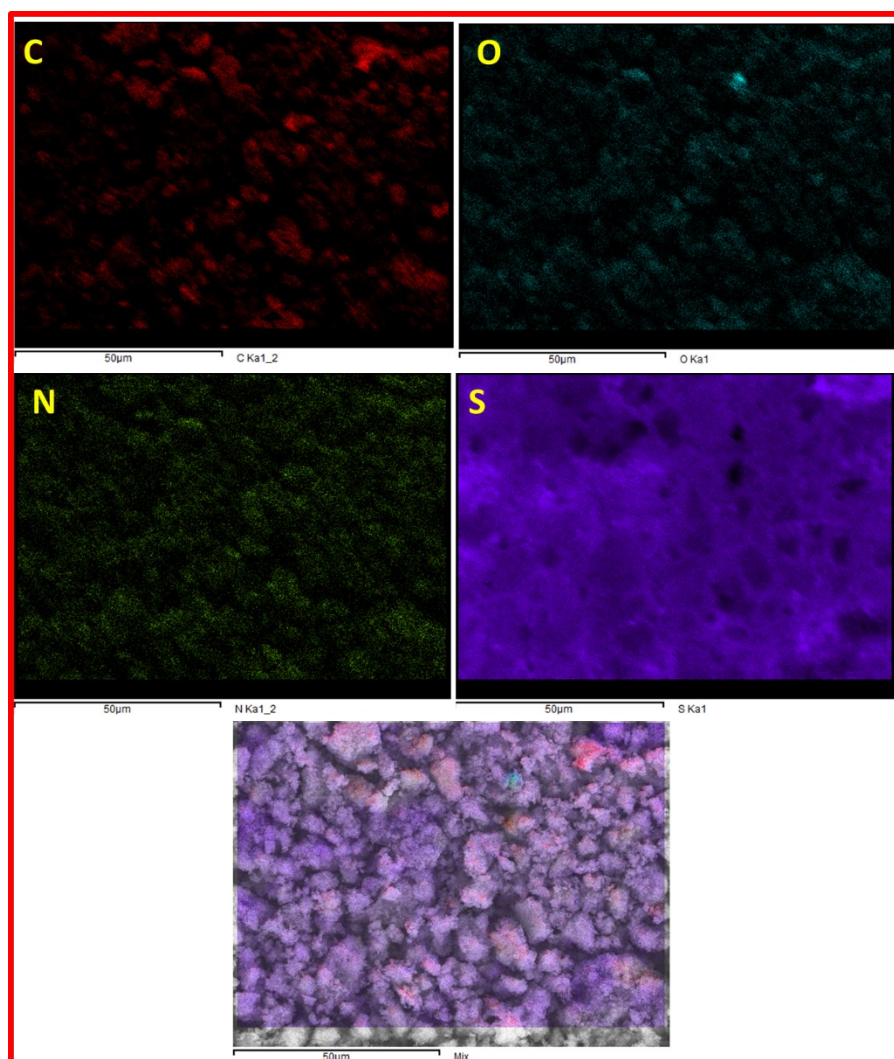


Figure S3. Selected area of CNFS-60 composite (chosen as a typical example) subjected to elemental mapping of carbon, nitrogen, oxygen, sulfur and cumulative elemental mapping image.

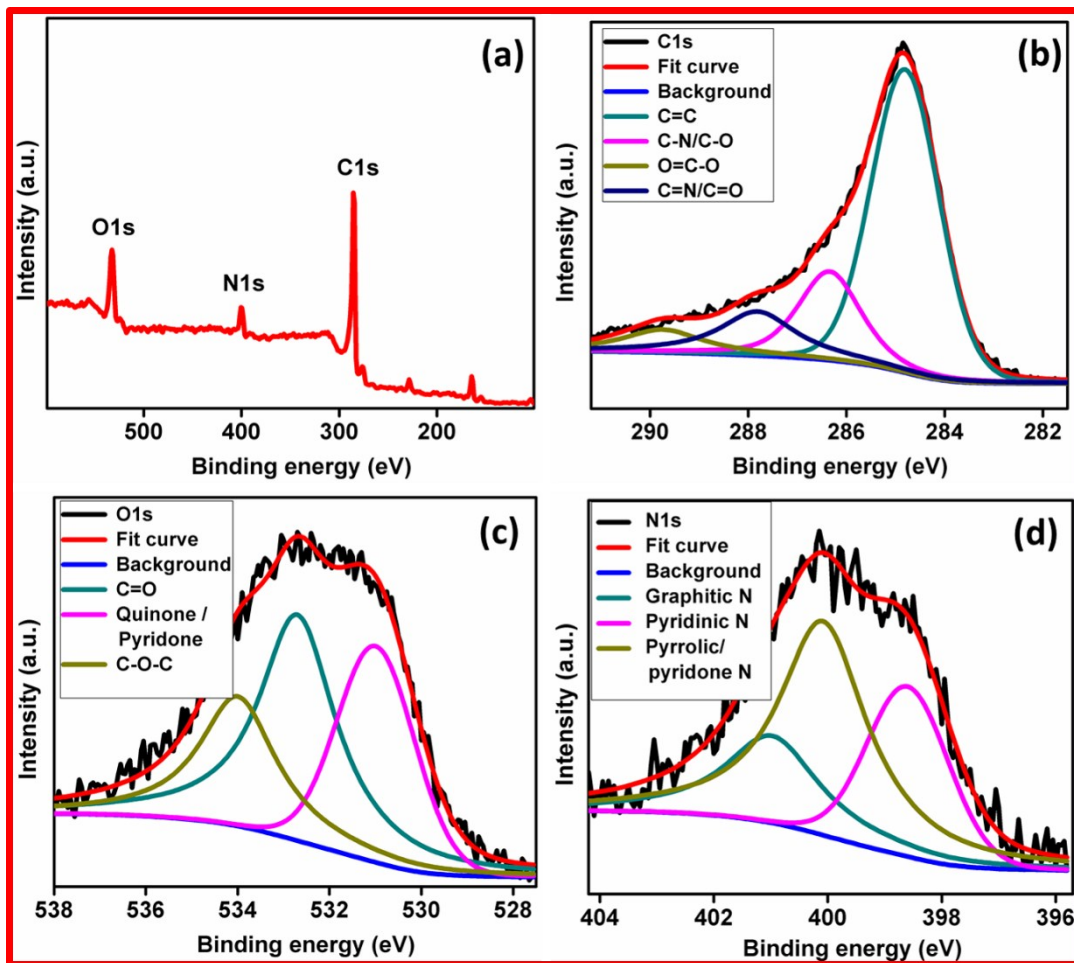


Figure S4. XPS survey spectrum (a) and deconvoluted spectra of C1s (b), O1s (c) and N1s (d) orbitals of CNF.

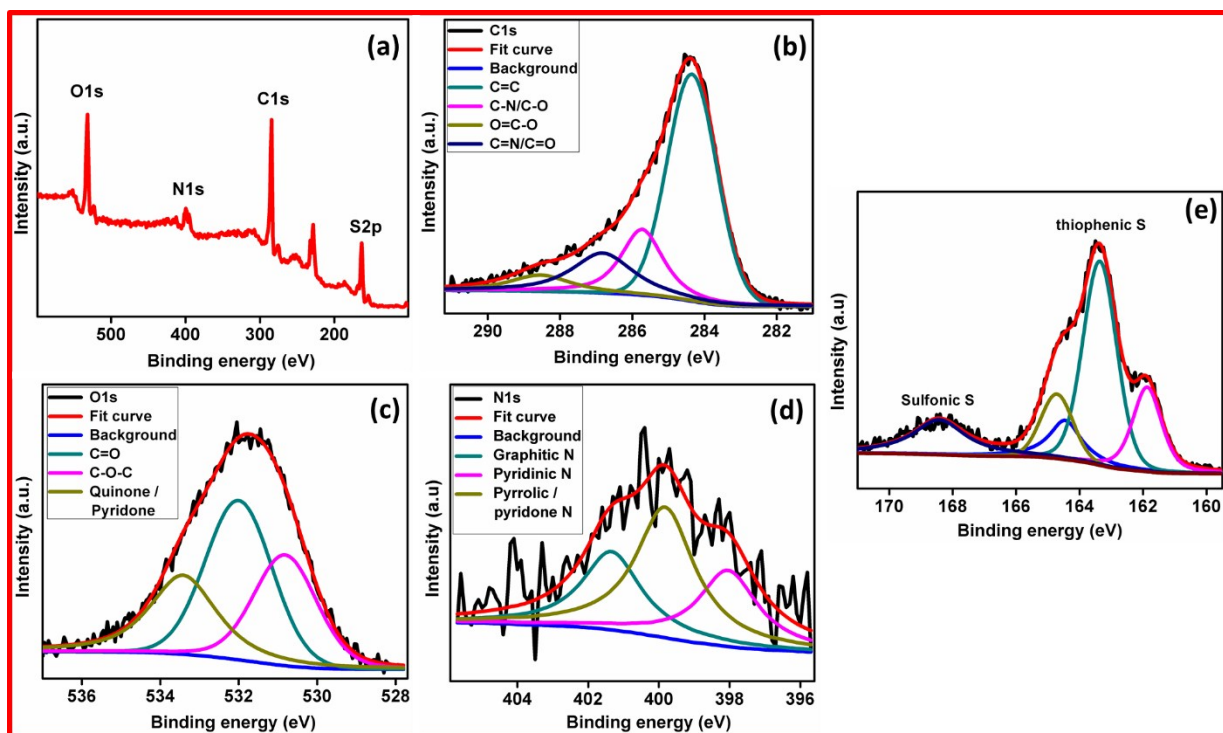


Figure S5. XPS survey spectrum (a) and deconvoluted spectra of C1s (b), O1s (c), N1s (d) and S2p (e) orbitals of CNFS-60 composite.

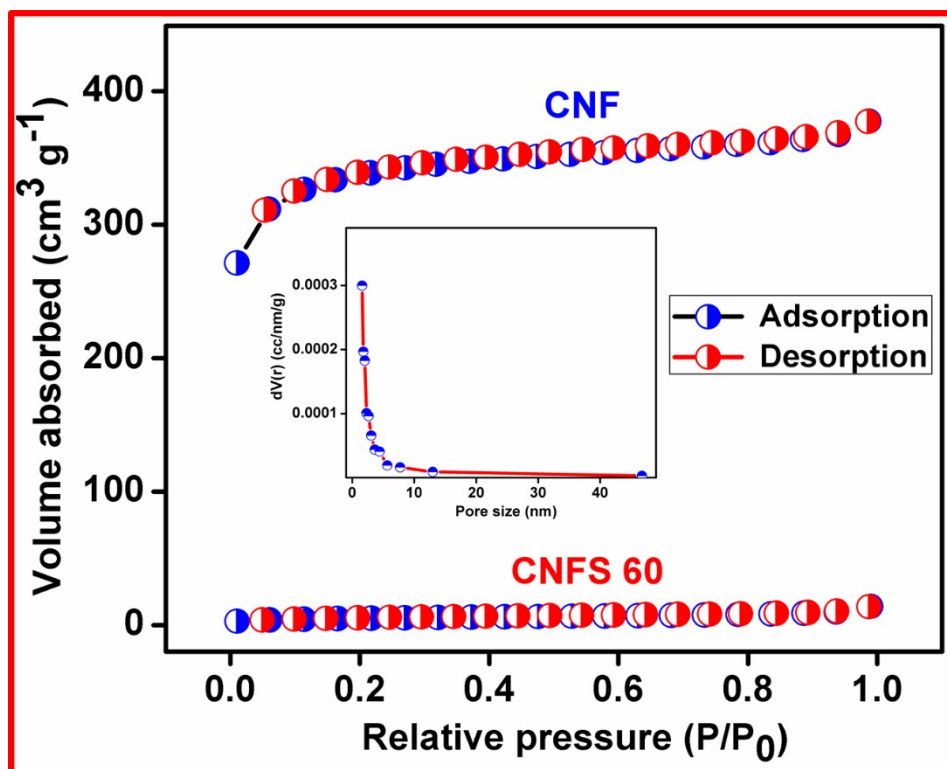


Figure S6. Nitrogen adsorption–desorption isotherm of CNF and CNFS-60 composite (inset corresponding to the pore volume distribution of CNF).

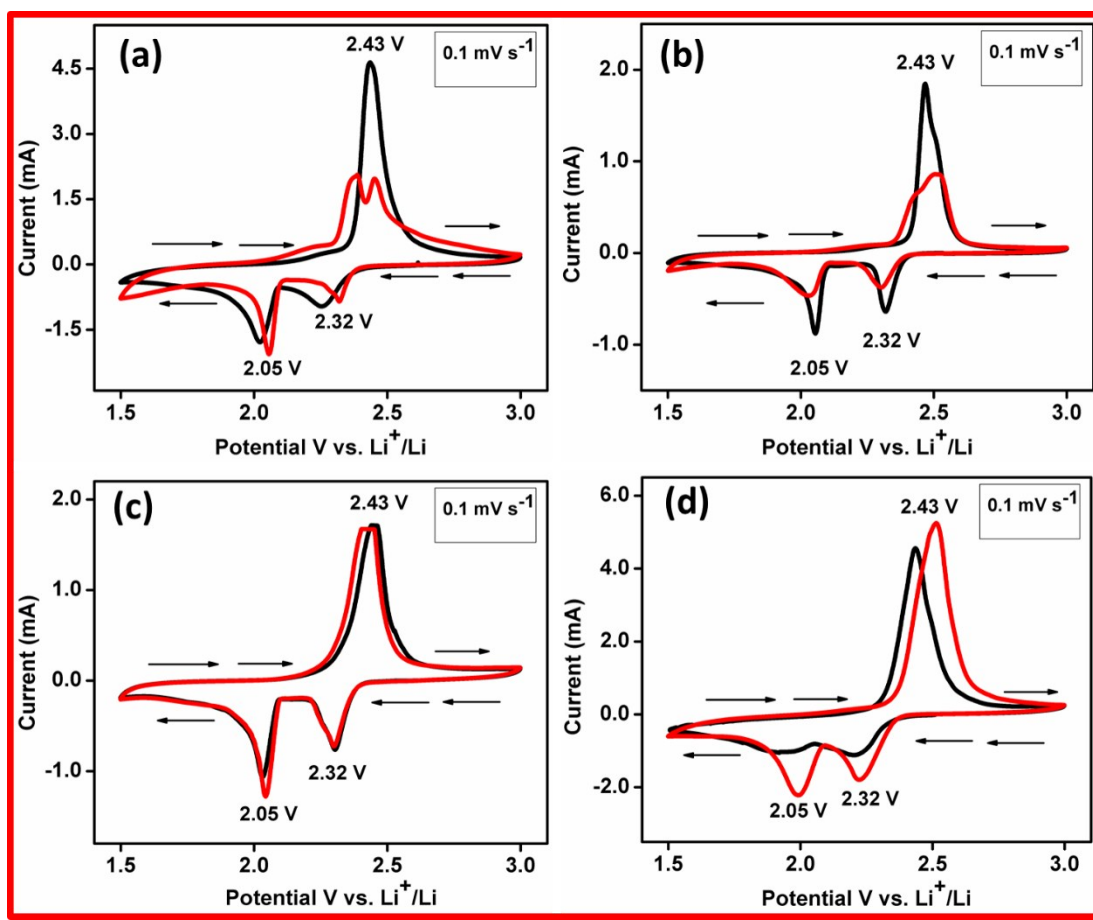


Figure S7. First and the tenth CV cycle behavior of CNFS-40 (a), CNFS-50 (b), CNFS-60 (c) and CNFS-70 (d) composite cathodes recorded at a scan rate of 0.1 mV s^{-1} .

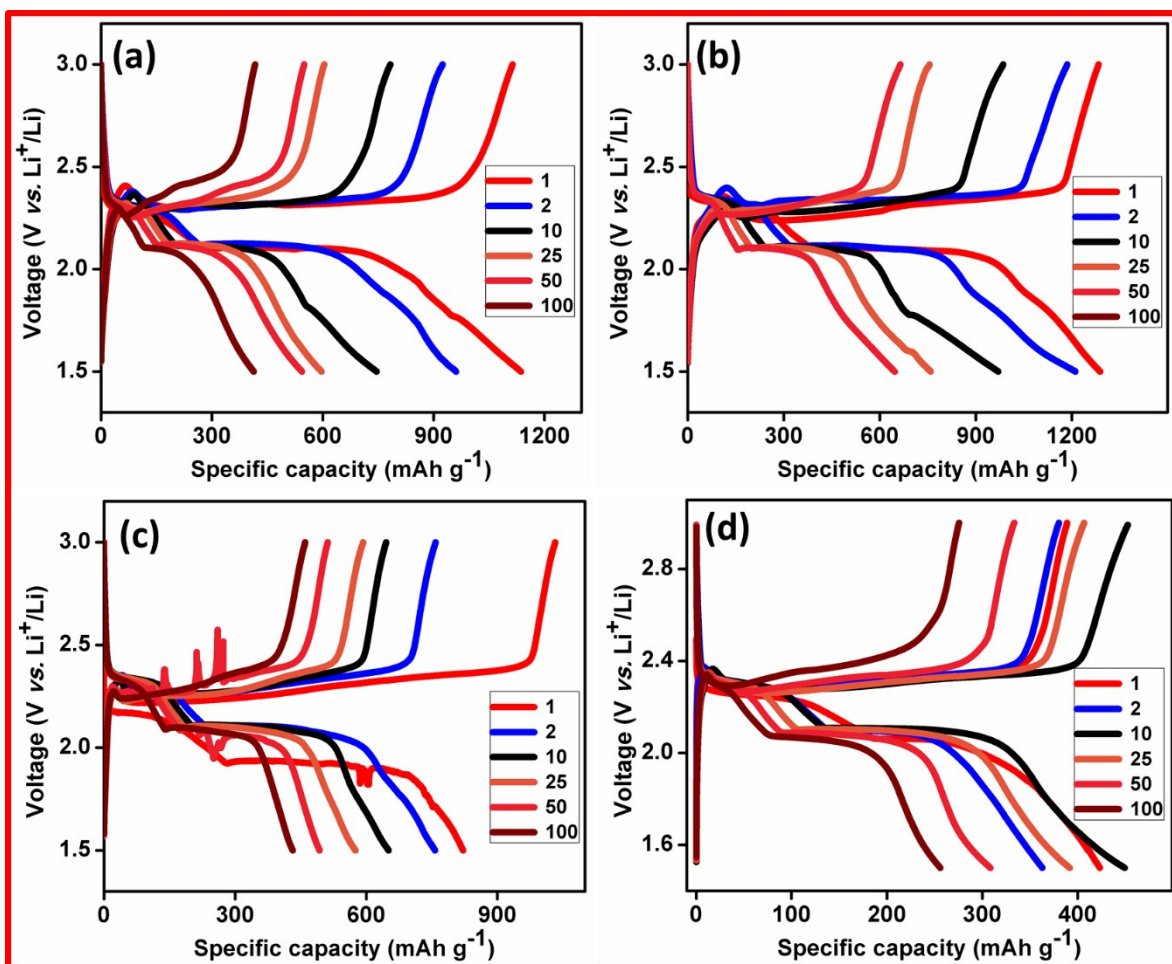


Figure S8. Charge-discharge profile of CNFS-40 (a), CNFS-50 (b), CNFS-60 (c) and CNFS-70 (d) composite cathodes.

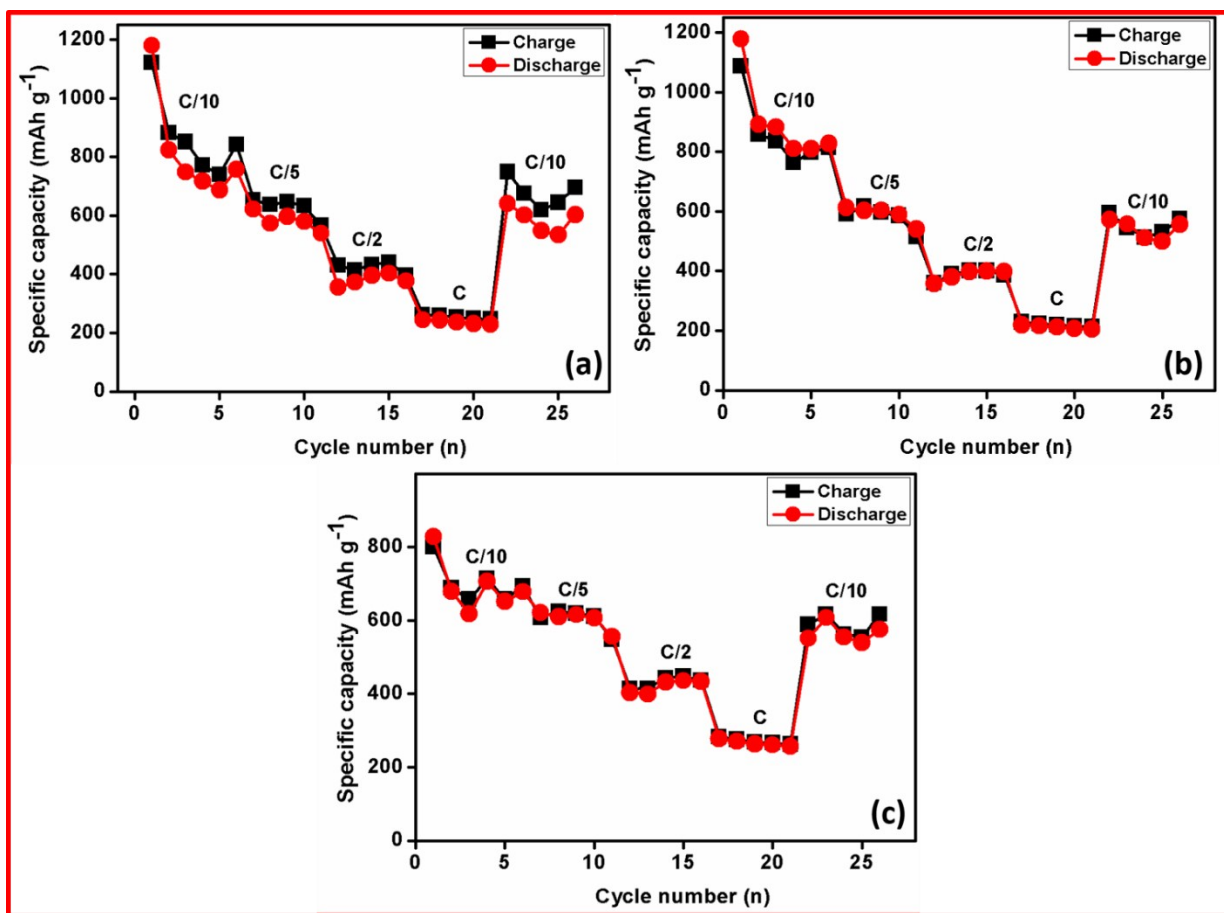


Figure S9. Rate capability behavior of CNFS-40 (a), CNFS-50 (b) and CNFS-60 (c) composite cathodes.

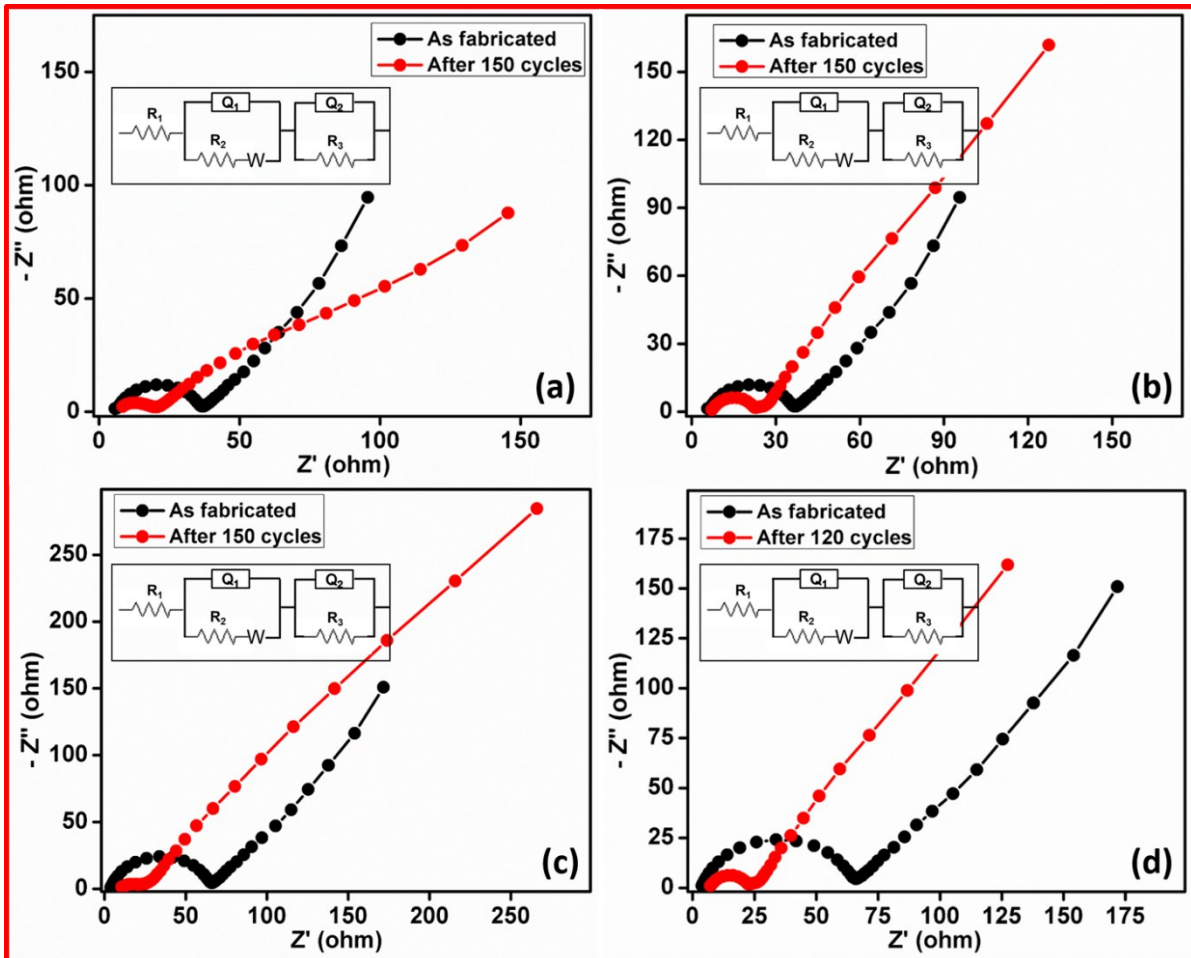


Figure S10. Electrochemical Impedance Spectroscopy results of CNFS-40 (a), CNFS-50 (b), CNFS-60 (c) and CNFS-70 (d) composite cathodes before and after cycling.

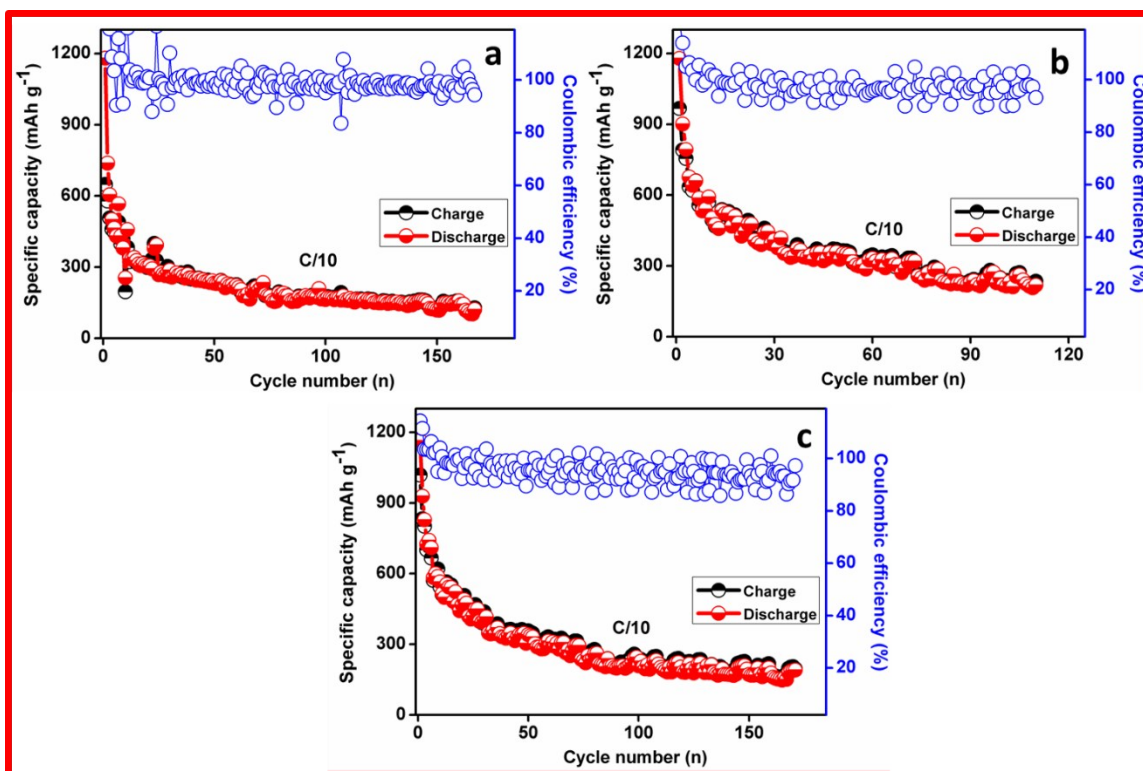


Figure S11. Cycling performance of CNFS-40 (a), CNFS-50 (b) and CNFS-60 (c) composite cathodes investigated at a current rate of C/10 with the addition of CNT as composite additive.

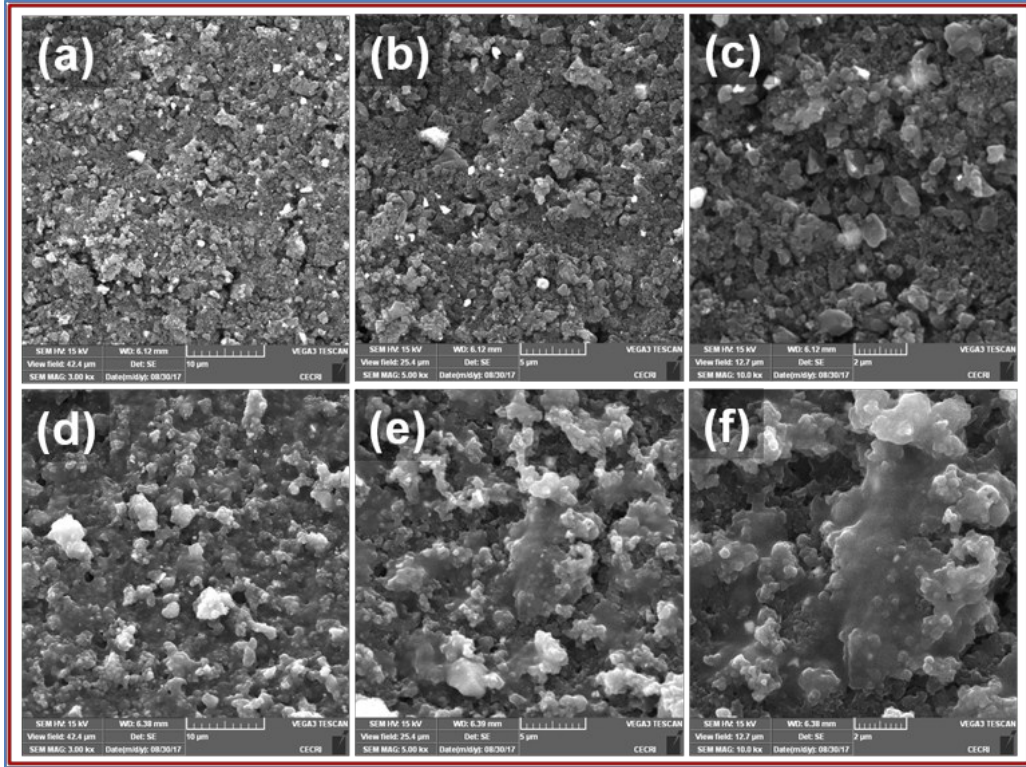


Figure S12. SEM images of CNF interlayer before (a-c) and after cycling (d-f), captured under different magnifications.

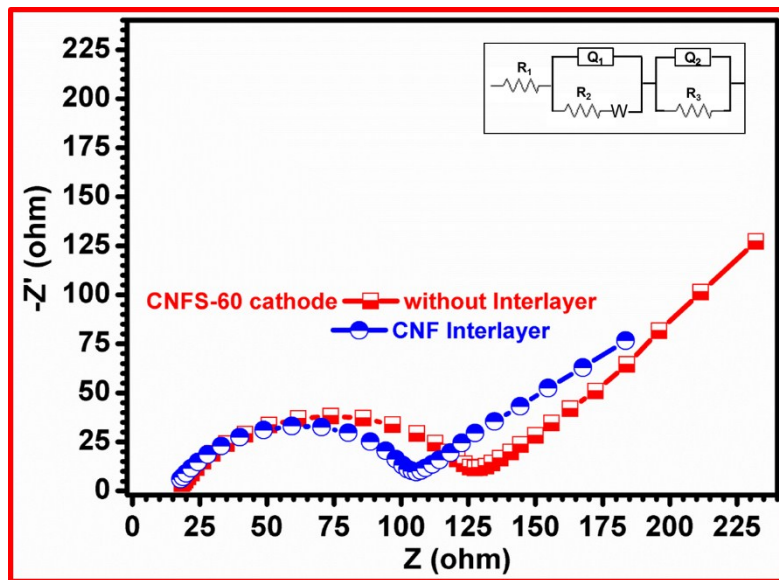


Figure S13. Electrochemical impedance behavior of CNFS-60 cathode with and without CNF interlayer.

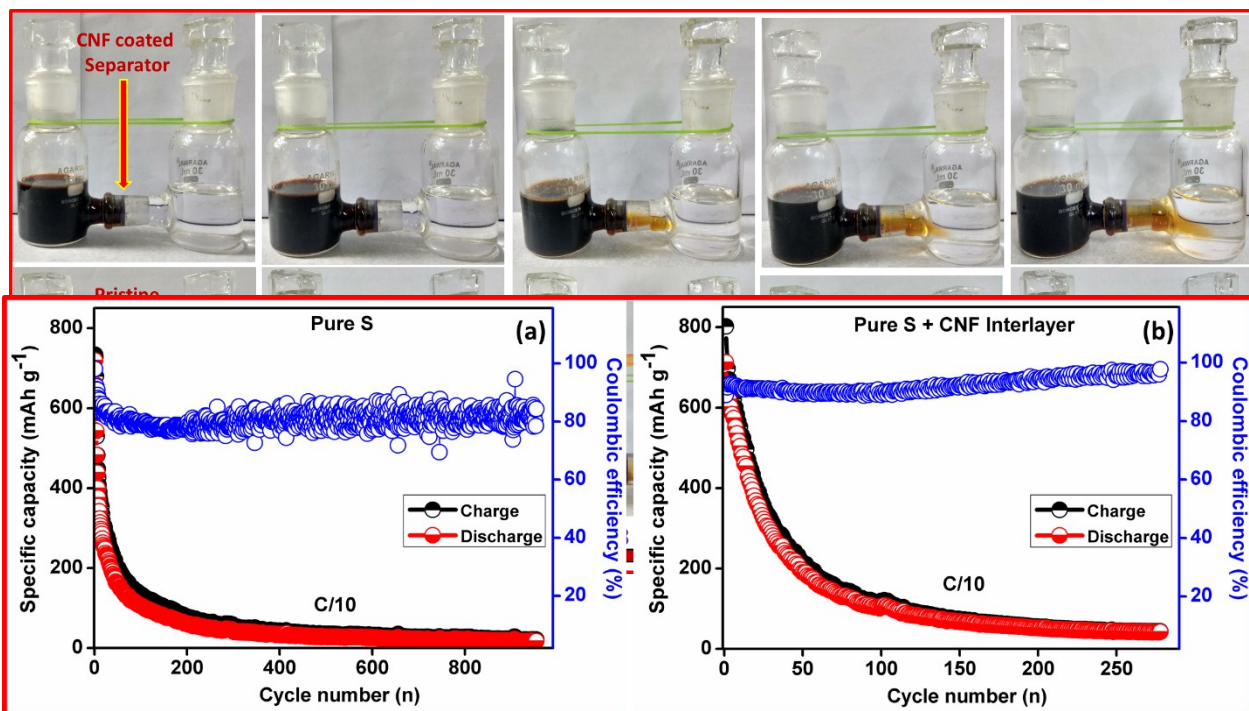


Figure S14. Photographs of glass cells with polysulfides (Li_2S_6) in DOL/DME solution and pure DOL/DME solvent in right and left chambers, respectively, separated by CNF interlayer coated separator (top row) and the pristine separator (bottom row).

Figure S15. Cycling performance of Pure S cathode with pristine separator (a) and Pure S cathode with CNF coated separator (b), investigated at a current rate of C/10.

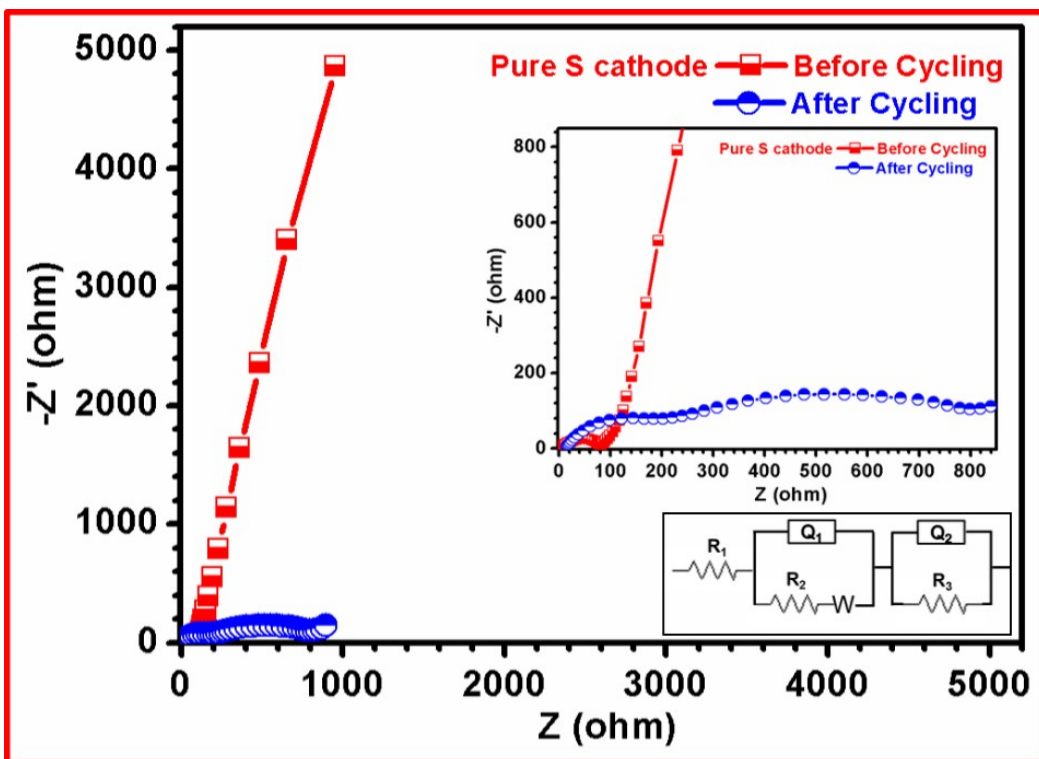


Figure S16. Electrochemical impedance spectroscopy results of pure S cathode with PP separator before and after cycling (50 cycles) (inset: enlarged EIS spectra).

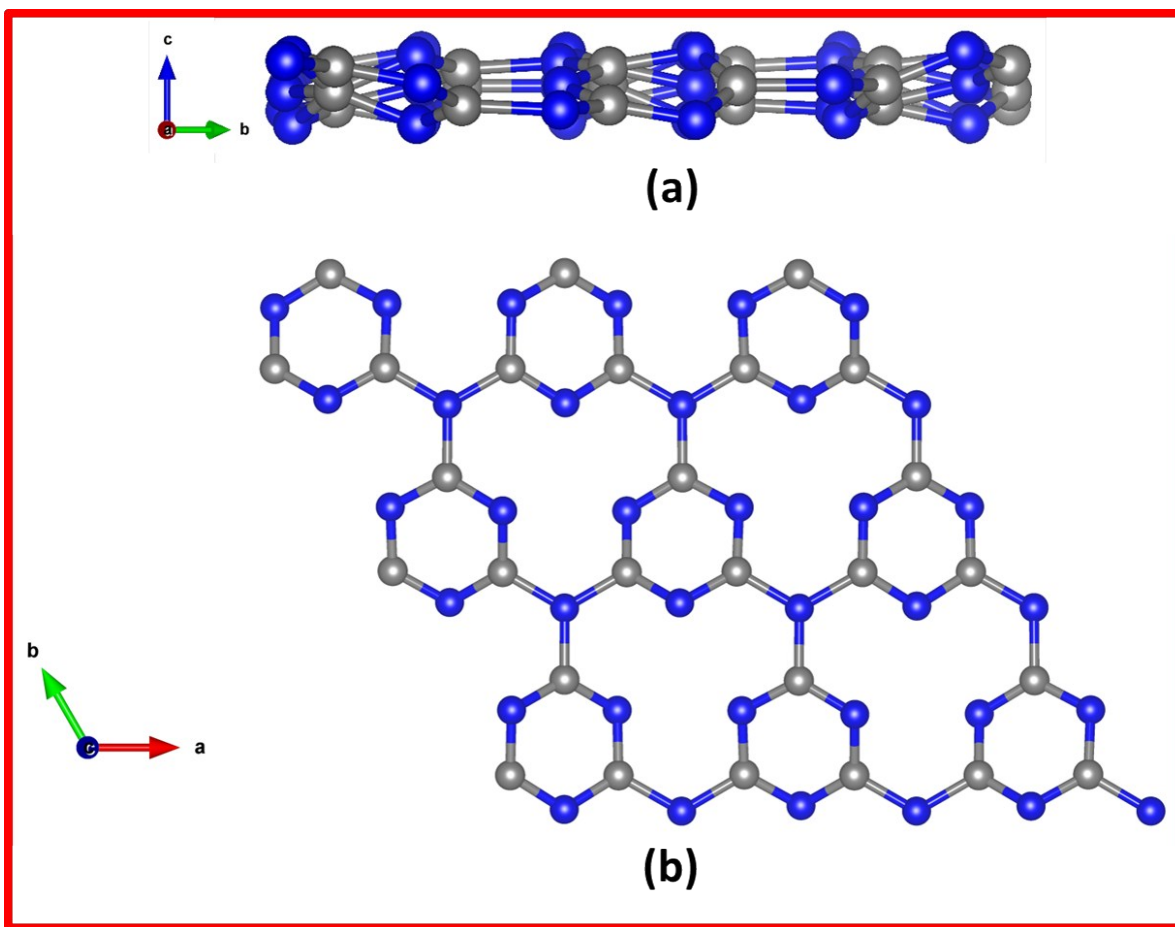


Figure S17. Lateral view (a) and Bird view (b) of CNF.

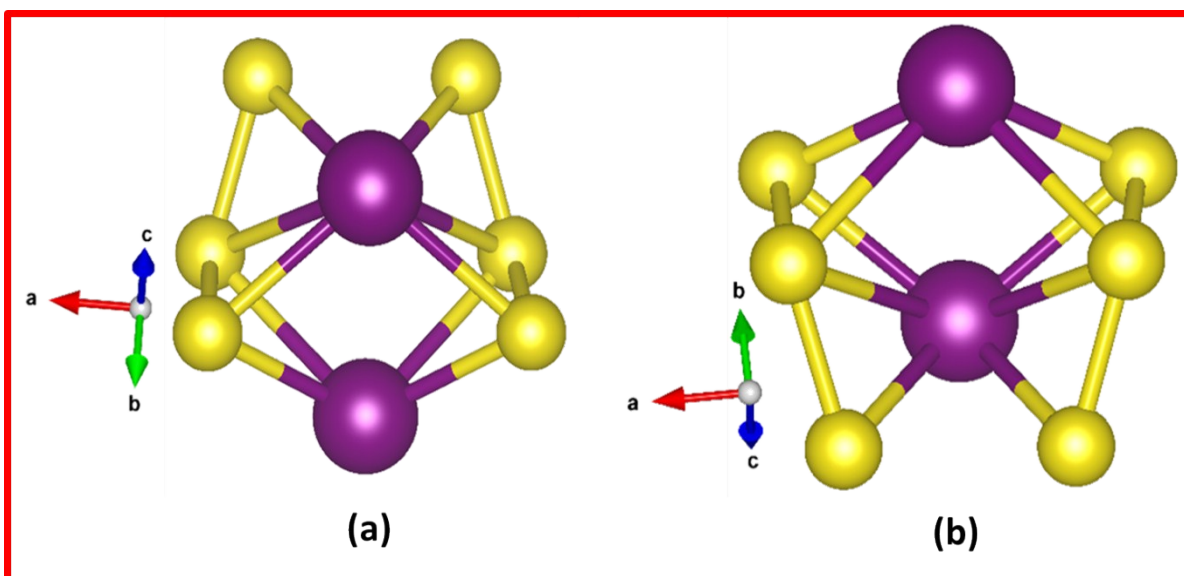


Figure S18. Two different orientations of Li₂S₆ cluster (a) and (b).

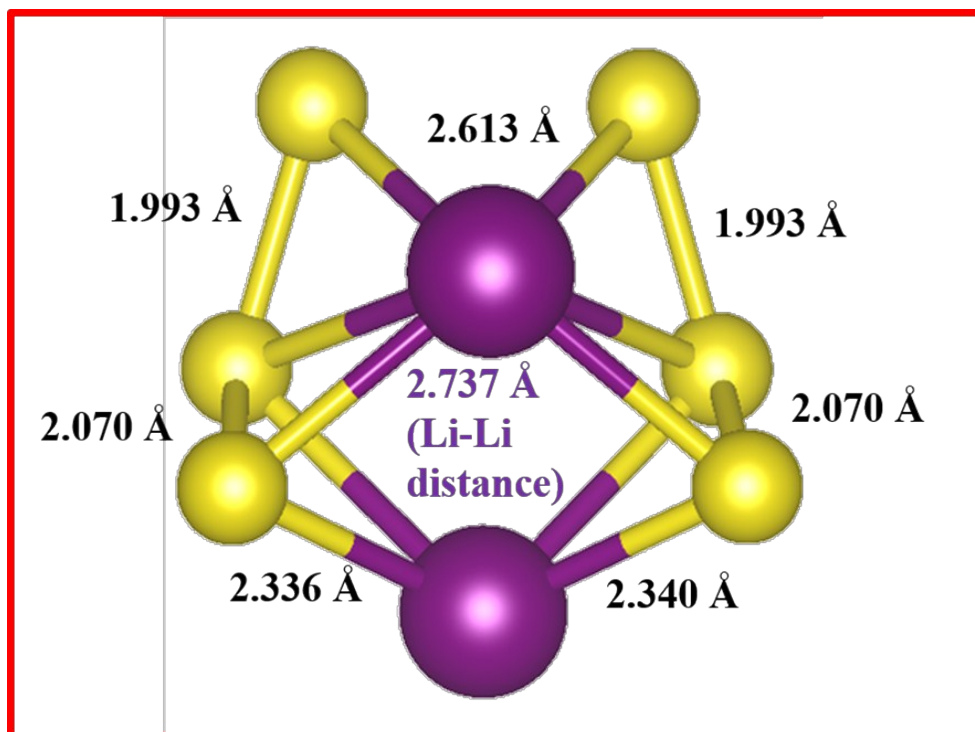


Figure S19. Lowest energy isomer of Li_2S_6 along with bond length analysis

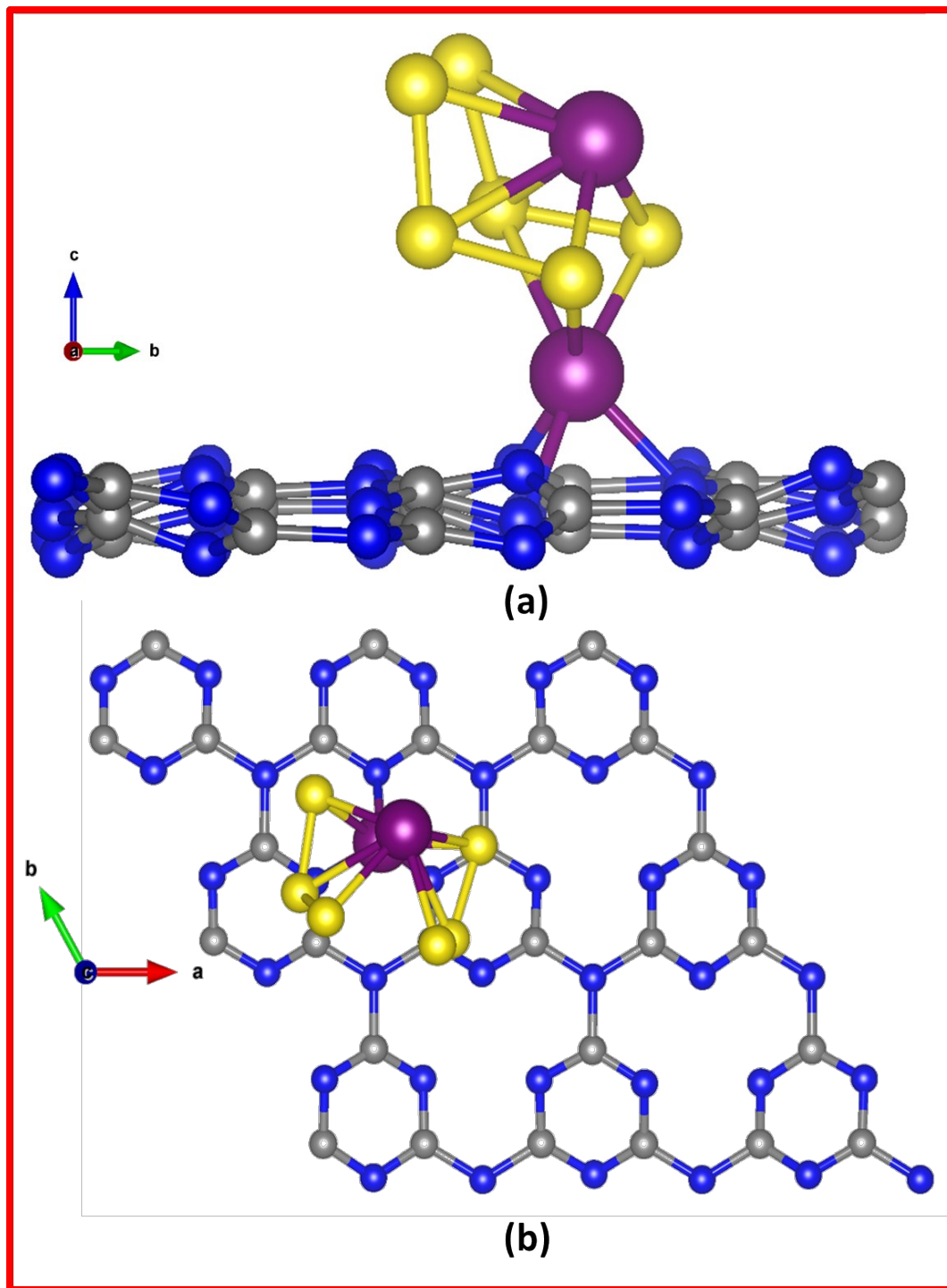


Figure S20. Lateral view (a) and Bird view (b) of CNF-Li₂S₆ composite.

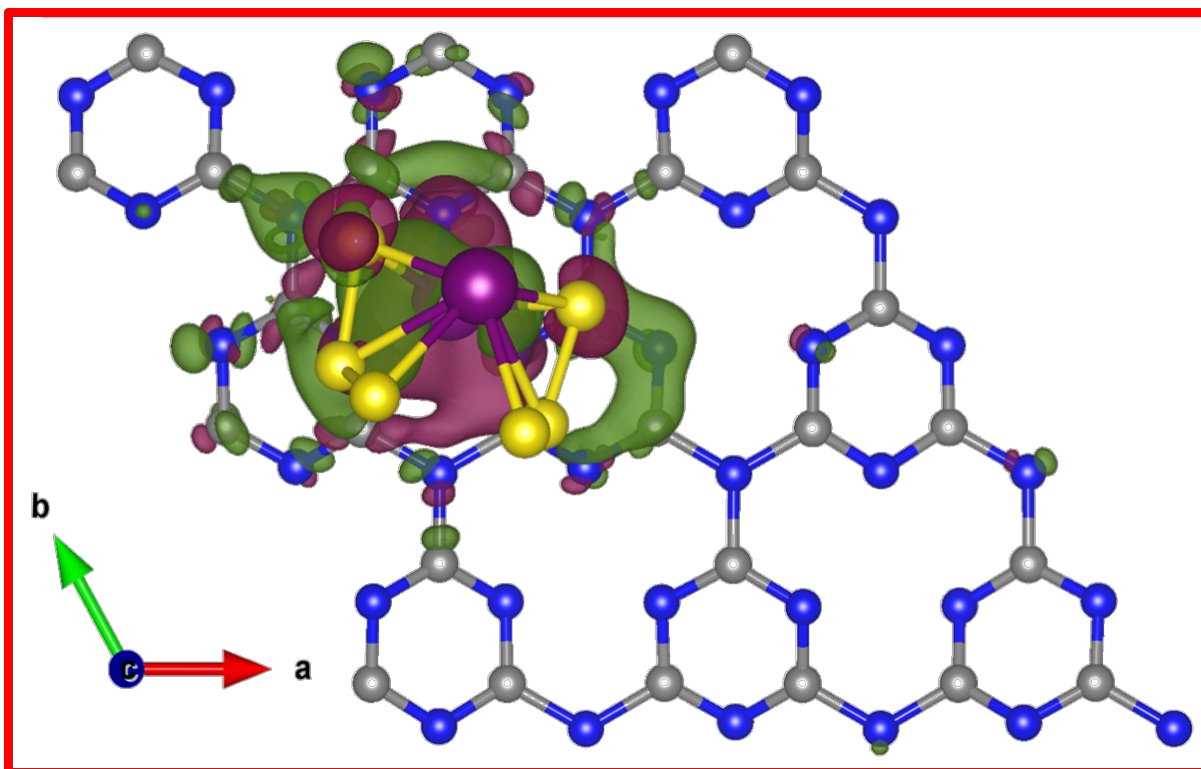


Figure S21. Bird view of charge density difference (CDD) of CNF-Li₂S₆ composite. Red contour indicates accumulation of charge and green shows depletion of charge region.

	hollow- mesoporous titania/CNTs	porous carbon													
11	Pure sulfur	MWCNTs	-	-	1000	150	950	150	621	300	-	-	-	-	39
12	Pure sulfur	Self-assembled MWCNTs	1100	1	1000	1	800	100	406 (3 A g ⁻¹)	3	-	-	-	-	40
13	Pure sulfur	Microporous carbon paper	-	-	-	-	1200	10	950	150	750	150	-	-	10
14	Pure sulfur	Nitrogen, sulfur- codoped graphene sponge	-	-	-	-	1400	10	1450	10	1000	100	780	10	41
15	Pure sulfur	Nitrogen-doped porous hollow carbon sphere	-	-	1250	5	1000	100	900	100	542	500	600	100	42
16	CNT-Sulfur	Permselective Graphene Oxide Membrane	850	5	800	5	750	5	700	5	600	5	-	-	43
17	Pure sulfur	Porouscarbonized graphene- embedded fungus film	-	-	-	-	1000	5	700	300	750	5	700	5	44
18	CNT-Sulfur	r-GO film	800 (0.2 A g ⁻¹)	5	750 (0.4 A g ⁻¹)	5	700 (0.8 A g ⁻¹)	5	600 (1 A g ⁻¹)	5	400 (1.2 A g ⁻¹)	5	-	-	45
19	Mesoporous	Graphite-modified	-	-	700	100	-	-	-	-	-	-	-	-	46

	carbon/sulfur composite	separator													
20	Ketjen Black/sulfur composite	Sulfonated reduced graphene oxide	-	-	1019	5	802	250	673	5	550	5	471 (4 C)	5	47
21	sulfur/carbon composite	Carbon Nanofiber	-	-	1400	28	-	-	-	-	-	-	-	-	48
22	Pure sulfur	Graphitic carbon fiber felt	-	-	1000	100	-	-	750	300	-	-	-	-	49
23	CNF	CNF	1361	7	954	7	790	7	686/437	7/300	571		443	7	This work
